

Recovery Study in Pure and Alloyed Aluminum Following Electron Irradiation*

A. SOSIN AND L. H. RACHAL

Atomics International, Division of North American Aviation, Inc., Canoga Park, California

(Received 21 January 1963)

Pure aluminum and slightly alloyed aluminum samples were bombarded with electrons near 4.2 and 78°K. The electrical resistivity increases introduced by the radiation were observed to recover in three stages: Stage I, below 50°K, Stage II centered at about 140°K, and Stage III, between 190 and 250°K. Stage III follows second-order kinetics with an activation energy of 0.45 ± 0.01 eV; Stage II follows close to first-order kinetics with an activation energy of 0.22 eV. The magnitude of Stage II depends sensitively on the amount and type of solute atoms in the lattice. Stage III is larger in alloyed aluminum than in pure aluminum and is shifted to lower temperature. The enhanced magnitude and the temperature shift are consistent with the observed second-order kinetics, indicating that the effect of alloying is to increase the number of defects which migrate in Stage III. A two-interstitial model, previously proposed to explain recovery in copper following irradiation, appears to account for these observations most satisfactorily.

INTRODUCTION

UNTIL recently, the majority of irradiation effects experiments in metals have been performed upon copper. The amount of attention devoted to this particular metal has been justified in part by the hope that a coherent description could be evolved which could then be taken over to other metals with a minimum of readjustment. This hope has been frustrated by two facts: no picture has been developed in copper sufficiently convincing to merit acceptance by all investigators and the extent of similarity between metals is still undetermined.

An important part of the difficulty in developing an acceptable model in copper has centered about the "Stage III dilemma." Most succinctly put, it appears at first glance that there is one more stage of recovery (of electrical resistivity, for example) following radiation than available defects. We return to this problem in more detail in the discussion.

The present study was designed to see if this dilemma exists in aluminum. The data described below leave little doubt that this is the case.

EXPERIMENTAL

The samples used in the bulk of this experiment consisted of 0.010-in. diam wires of aluminum or Al+0.1 at.% Zn mounted in a copper box as shown in Fig. 1. Four lengths, each approximately 1.2 cm long, resulted from weaving the single wire as indicated from, posts on two five-post hollow metal-to-glass seals. Copper lead-ins were soldered into each metal tube and the sample soldered to the lead-ins. The samples were enclosed by sealing a copper foil on top of the box with Dow-Corning vacuum grease.

During irradiation, liquid nitrogen was passed around the box. During measurements, the entire box was submerged in liquid helium. During annealing, the box was submerged in a massive bath of precooled and thermally regulated petroleum ether or propane.

*This work was supported by the U. S. Atomic Energy Commission.

Prior to irradiation, the sample wires were annealed to 400°C in vacuo. They were then mounted with care to minimize deformation. Finally, they were annealed in place at about 250°C in air.

The measurements were of a standard potentiometric variety, using a measuring current of 1.0 A. The current was controlled to about one part in 10^5 . The electron current density during irradiation was maintained below $20 \mu\text{A}/\text{cm}^2$.

The residual resistivities, ρ_0 , of the samples were about 2 to $3 \times 10^{-9} \Omega\text{-cm}$ for the pure aluminum wires (nominally 99.9999% pure in the as-supplied condition) and $4.8 \times 10^{-8} \Omega\text{-cm}$ for the Al+0.1 at.% Zn alloy. This last value is in fair agreement with the value given by Vassel.¹

The absolute values of ρ are limited by geometry uncertainty and can be determined to within about $\pm 5\%$. Furthermore, the precision of electron flux measurements is limited by electron scattering, mainly on passing through two metal foils before striking the samples (the foil at the exit of the accelerator and the

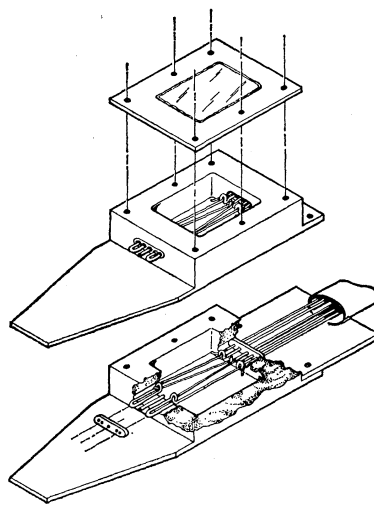


FIG. 1. Schematic drawing of sample holder.

¹ C. R. Vassel, *J. Phys. Chem. Solids* 7, 90 (1958).

foil covering the sample box). Thus, the damage rates, $d\rho/d\phi$ ($\Omega\text{-cm}$ per electron/ cm^2), are probably known to a precision of $\pm 10\%$. However, precision in the relative values of resistivity—the most important factor in these experiments—is probably better than $\pm 0.01\%$.

The accelerating voltage for the electrons used in the irradiations at liquid nitrogen was 1.25 MeV. However, the energy was degraded on passage of the electrons through two copper foils and a small amount of air so that the incident energy was approximately 1.1 MeV. Further degradation of energy occurred passing through the sample. The effective energy was, therefore, about 1.0 MeV.

One set of measurements is also included in this report in which 0.002-in. diam wires were bombarded in vacuo near 4.2°K. The experimental arrangements and techniques have been described elsewhere.²

RESULTS AND DISCUSSION

A. Stage III

Figure 2 shows the results of an electron irradiation near 4.2°K of pure Al, Al+0.1 at.% Cu, and Al+0.1 at.% Zn. This study is not complete. These results are included to provide background information for the experiments subsequently described. The features borne out by this figure which are pertinent to the present results are:

- The presence of Stage I ($< 55^\circ\text{K}$) recovery. This stage appears to be at least qualitatively similar to that observed in Cu.
- The suppression of Stage I recovery by the addition of Zn or Cu.
- The different character of Stage II (between 55 and 175°K) recovery in the various samples.
- The shift to lower temperature of the Stage III ($\sim 250^\circ\text{K}$) recovery with alloying. It should be noted that all four samples were irradiated and annealed together.

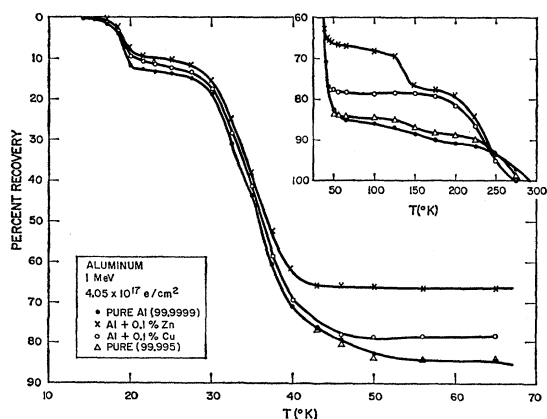


FIG. 2. Isochronal recovery of the electrical resistivity of pure Al following irradiation near 4.2°K. The time at each temperature is 5 min.

² A. Sosin and H. H. Neely, Rev. Sci. Instr. 32, 999 (1961).

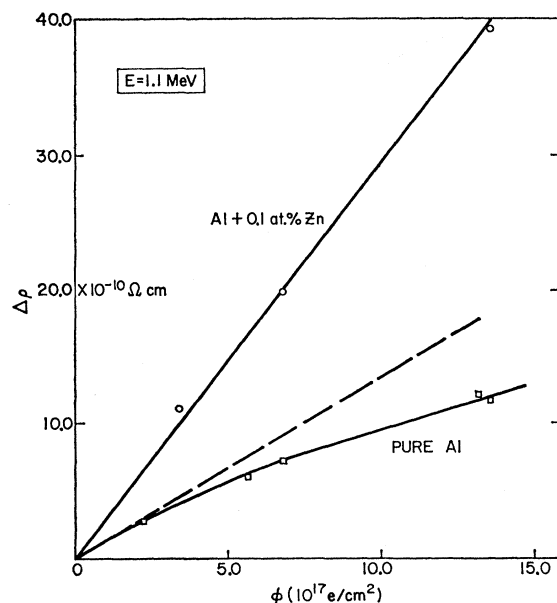


FIG. 3. Exposure curve for samples irradiated by 1.1 MeV (incidence energy) electrons at 80°K. The straight lines correspond to the approximate exposure curves expected from irradiation at 4.2°K (see Fig. 2).

We now turn to the main results of this study. Figure 3 shows the “exposure curves” for the two materials irradiated at 80°K. The dashed line drawn in the figure corresponds to the approximate damage rate which one would predict in pure aluminum on the basis of Fig. 2 (i.e., from the resistivity which remains after Stage I annealing). The damage rate for the alloy appears to be in good agreement with the results from Fig. 2.

In Fig. 4 are presented results of two sets of isochronal annealing studies. The difference between the initial values in this figure and the end values in Fig. 3 represents the extent of Stage II anneal (see also Fig. 2). It can be seen that the cross-over at the end of the curves is an indication of the extent of nonreproducibility between successive experiments. This is further demonstrated by noting the final extent of recovery in Fig. 2.

Isothermal data are presented in Fig. 5. These data are replotted in Fig. 6. The linearity of the data plotted in this manner indicated that Stage III follows second-order chemical rate kinetics. Thus, the time rate of decay of the concentration c of migrating defects is

$$dc/dt = -Kc^2, \quad (1)$$

where

$$K = \nu \exp(-E_{III}/kT) \quad (2)$$

and

$$\Delta\rho = \rho_F c. \quad (3)$$

In these expressions, $\Delta\rho$ is the resistivity increment due to the defects involved in Stage III recovery, ν is a

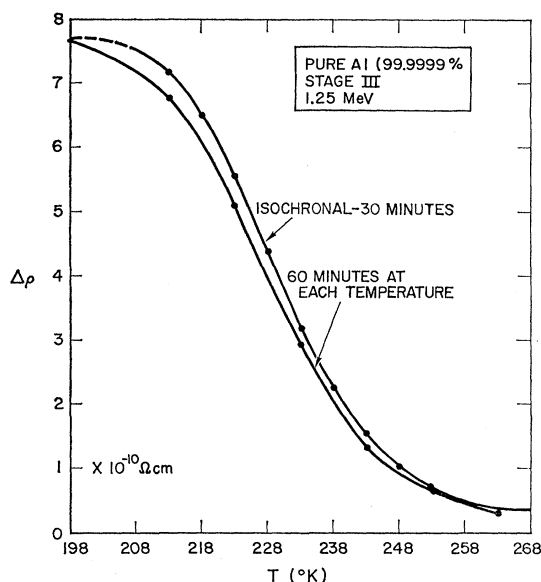


FIG. 4. Isochronal recovery of the electrical resistivity of pure Al in the Stage III temperature region.

defect jump attempt frequency ($\sim 10^{13} \text{ sec}^{-1}$), E_{III} is the rate governing activation energy, and ρ_F is the resistivity per unit concentration of defects which are eliminated during Stage III recovery. The subscript F is written in anticipation of our conclusion that the main process involves vacancy—interstitial recombination; then ρ_F is the resistivity per unit concentration of Frenkel pairs, which we shall take, somewhat arbitrarily, to be $3 \times 10^{-4} \Omega\text{-cm}$.

The data of Figs. 4 and 5 are combined in Fig. 7 using the method of Meechan and Brinkman.³ This yields the activation energy: $E_{III} = (0.448 \pm 0.009) \text{ eV}$. Note that the vertical shift between the two lines is $(\ln 60 - \ln 30)$. This is also in accord with Brinkman's analysis since the (total) time at each temperature was either 60 or 30 min, as indicated.

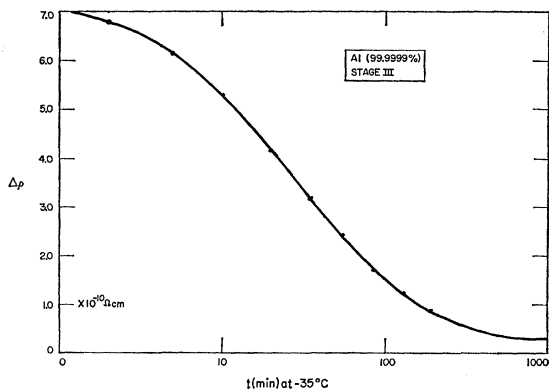


FIG. 5. Isothermal recovery of the electrical resistivity of pure Al in the Stage III temperature region.

³ C. J. Meechan and J. A. Brinkman, Phys. Rev. **103**, 1193 (1956).

Figure 6 indicates that second-order kinetics are obeyed for at least 200 min at -35°C . This represents about two decades in time since the first measurement was made after 2 min. Figure 8 indicates that second-order kinetics dominates the process over about $3\frac{1}{2}$ decades in time. The technique used to deduce Fig. 8 is discussed in detail in the Appendix. It is significant to note that a second-order process goes from 10 to 90% completion in approximately two decades of time, whereas the portion of recovery analyzed in Fig. 8 is about 93%. Thus, Fig. 8 is a particularly rigid test, both of the constancy of the activation energy, used directly in the analysis leading to the figure, and of the second-order kinetics.

We now turn to the behavior of the resistivity of $\text{Al}+0.1 \text{ at.}\% \text{ Zn}$. The results of an isochronal annealing experiment are presented in Fig. 9; isothermal annealing data are shown in Fig. 10. The isothermal data are replotted in Fig. 11 in a manner again demonstrating second-order kinetics. Both isothermal and isochronal measurement are combined in Fig. 12, following the method of Meechan and Brinkman, to yield the activa-

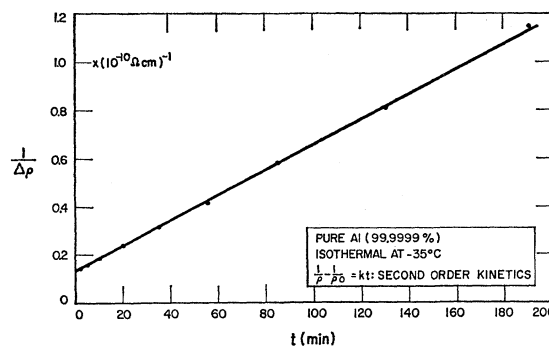


FIG. 6. A replot of the data of Fig. 5. The linearity in this plot indicates that the recovery process follows second-order kinetics.

tion energy. The energy deduced in this manner agrees with the value determined in pure Al.

If we assume that Stage III is due to the migration and annihilation of the same defect in pure aluminum and the alloy, we may explain the fact that Stage III in the alloy occurs at lower temperatures than in the pure material. The temperature shift—approximately 13°K in the position of the “center temperatures” (i.e., the temperature in the tempering curve, Fig. 9, at which the inflection occurs)—is directly related to the different concentration of defects involved in the two cases, even though the amount of irradiation was nearly equal in both cases. An analysis which applies to this case has also been given by Meechan and Brinkman. They give the following expression:

$$c_0 \nu A^{-1} \exp[-E/kT_c] = T_c^{-1} \left[\frac{2}{E/kT_c} - \frac{1}{1+E/kT_c} \right]^{-1}, \quad (4)$$

where c_0 denotes the total concentration of defects involved in the recovery stage, T_c is the center temperature, ν is the vibrational frequency, and A is the rate of temperature rise, assumed constant. Inserting values of T_c for the pure aluminum and alloy samples of 229 ± 1 and $216 \pm 1^\circ\text{K}$, respectively, this expression predicts a concentration ratio for the two samples of 3.5 ± 0.7 . Experimentally, the concentration ratio is approximately 3.4.

B. Stage II

We have also studied the recovery of electrical resistivity in Stage II in Al+0.1 at.% Zn in some detail.

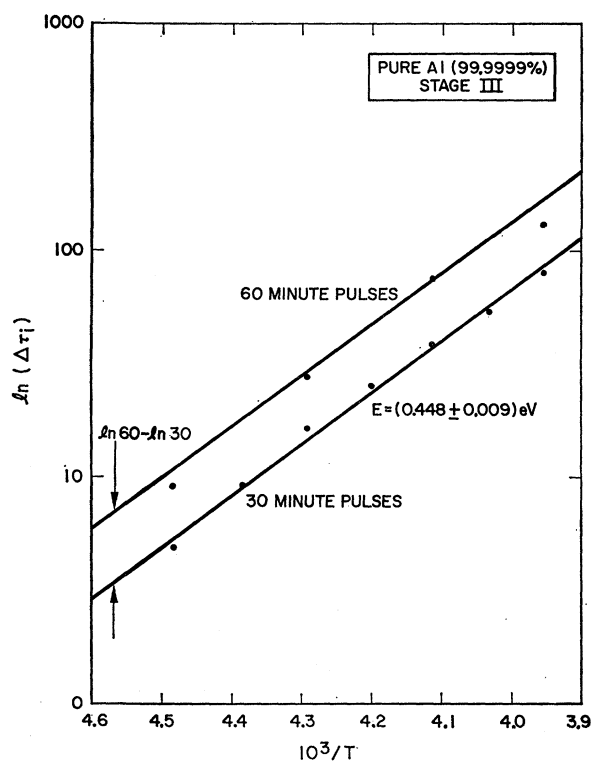


FIG. 7. A determination of the activation energy governing recovery of the electrical resistivity of pure aluminum in Stage III. The curves are derived from the data in Figs. 4 and 5.

First the isochronal data points of Fig. 9 in the Stage II temperature region were analyzed using the time-correction procedure outlined in the Appendix. The results indicate that Stage II obeys first-order kinetics. This is demonstrated first in Fig. 13 where a plot of $\ln[\ln(\rho_0/\rho)]$ vs $1/T$ yields a straight line (ρ_0 is the resistivity at the beginning of the stage—i.e., the first data point). The slope of this line indicates an activation energy $E_{II} = 0.225$ eV.

The experiment leading to Fig. 9 was actually of the sequential isothermal variety. Four measurements, at

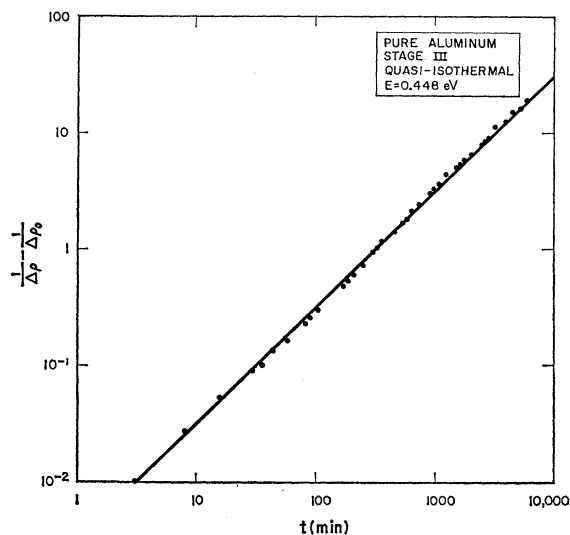


FIG. 8. A second demonstration of the second-order kinetics governing Stage III recovery in pure Al. The details of the method used are described in the text. The units of the ordinate are $10^9 (\Omega\text{-cm})^{-1}$. The units of the abscissa are minutes at 213°K .

different times, were made at each temperature. Only the last measurements, after 30 min of annealing at each temperature, are shown in Fig. 9. Having deduced the activation energy, all the data points may be used with the time-correction procedure to construct an extended isothermal (see Fig. 14). Finally the isothermal data are replotted in Fig. 15 as $\ln(\rho/\rho_0)$ vs $\ln t$. The resulting straight line with unit slope again demonstrates the precision with which first-order kinetics are obeyed.

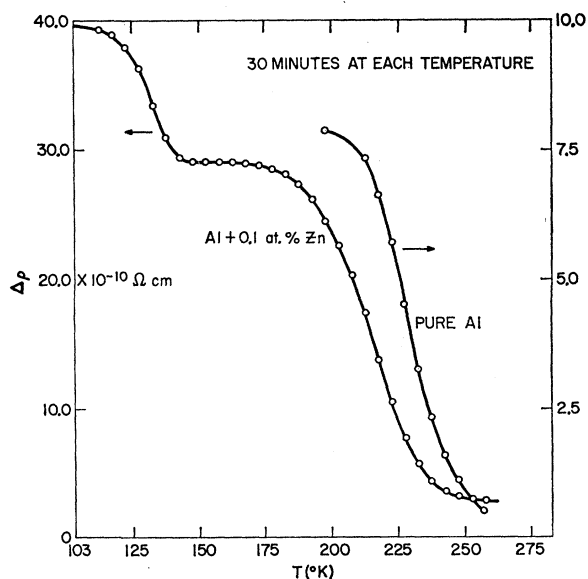


FIG. 9. Isochronal recovery of the electrical resistivity of pure Al and Al+0.1 at.% Zn following electron irradiation at 80°K .

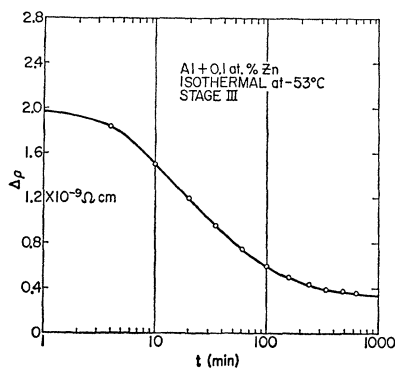


FIG. 10. Isothermal recovery of the electrical resistivity of Al+0.1 at.% Zn in the Stage III temperature region.

DISCUSSION

Some implications of the data presented herein are quite clear. Stage III recovery is very similar in aluminum and copper³ or nickel.⁴ Furthermore, Stage I recovery appears to be qualitatively similar in aluminum and copper.^{5,6} Interstitial atoms are presumed to migrate in Stage I in both cases and, in the main, recombine with vacancies. It is reasonable to assume that recombination of close interstitial-vacancy pairs occurs in the earlier part of Stage I and that interstitial-vacancy recombination is less correlated as the recovery proceeds. The fact that full recovery is not achieved in Stage I (in either aluminum or copper) indicates either that some of the interstitials which are mobile in Stage I are immobilized in some unspecified manner rather than being annihilated at vacant lattice sites or that some of the interstitials are inherently immobile in Stage I. The choice between these two alternatives remains a matter of discussion.

It is also clear that the presence of zinc or copper

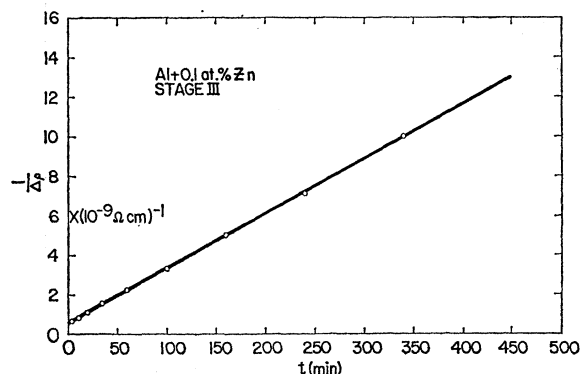


FIG. 11. A replot of the data of Fig. 10. The linearity in this plot indicates that the recovery process follows second-order kinetics.

⁴ A. Sosin and J. A. Brinkman, *Acta Met.* **7**, 478 (1959).

⁵ J. W. Corbett and R. M. Walker, *Phys. Rev.* **114**, 1452, 1460 (1959).

⁶ A. Sosin, *Phys. Rev.* **126**, 1698 (1962).

atoms suppresses recovery in Stage I. It is reasonable to assume that this suppression results, at least in part, from the "trapping" of interstitials by foreign atoms and that "detrapping" occurs in Stage II. This follows from the observation that Stage II is a first-order process in Al+0.1 at.% Zn (see the subsequent discussion). The annealing in Stage II in the "pure" samples is probably related to the presence of several types of trace impurities, leading to a spectrum of first-order processes.

The first significantly unresolved question is: Why is there no Stage II recovery in Al+0.1 at.% Cu? Our proposed answer to this question requires some discussion of the nature of the damage which remains in pure

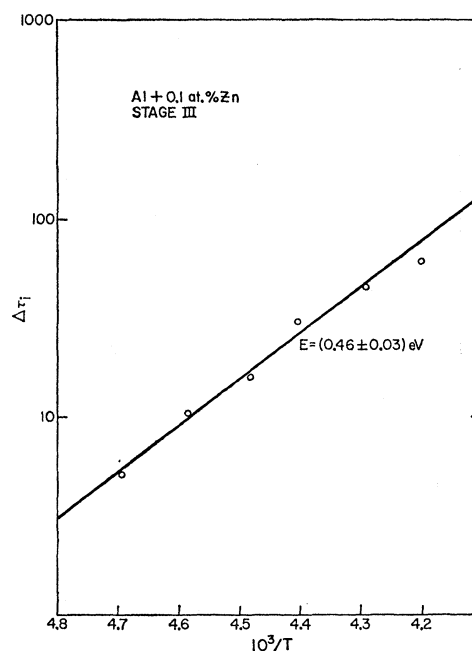


FIG. 12. A determination of the activation energy governing recovery of the electrical resistivity in Stage III in Al+0.1 at.% Zn.

Al after Stage I recovery is complete. We shall adopt a two-interstitial model in this paper.

The two-interstitial model which we explore here was previously proposed for the recovery of electrical resistivity following irradiation of Cu.^{7,8} Briefly, it was proposed that a $\langle 110 \rangle$ interstitial configuration (a crowdion) is mobile in Stage I, whereas a second form, a $\langle 100 \rangle$ configuration, is mobile in Stage III. Stage II—following irradiation—is presumed to be due mainly to the release of crowdions from traps, usually near impurity atoms. Stage IV, occurring above room temperature in Cu, is due to vacancy migration. The reader is

⁷ C. J. Meechan, A. Sosin, and J. A. Brinkman, *Phys. Rev.* **120**, 411 (1960).

⁸ A. Seeger, *Radiation Damage in Solids* (International Atomic Energy Agency, Vienna, 1962).

referred to the previous reports^{7,8} for a more detailed account of this model.

In the two-interstitial model, the evident suppression of Stage I recovery due to foreign atoms is due to two effects. The first one is dynamic. Crowdions are ejected relatively long distances through the lattice during irradiation. It then appears that crowdions' dynamic paths are frequently sufficiently perturbed by the presence of foreign atoms that interstitials are defocused from mass transport along the $\langle 110 \rangle$ direction and come to rest in $\langle 100 \rangle$ configurations. Thus, the relative number of interstitials which are mobile in Stage I is reduced in the alloyed material.

The second effect which leads to suppression is trapping during thermal migration. Here we conclude

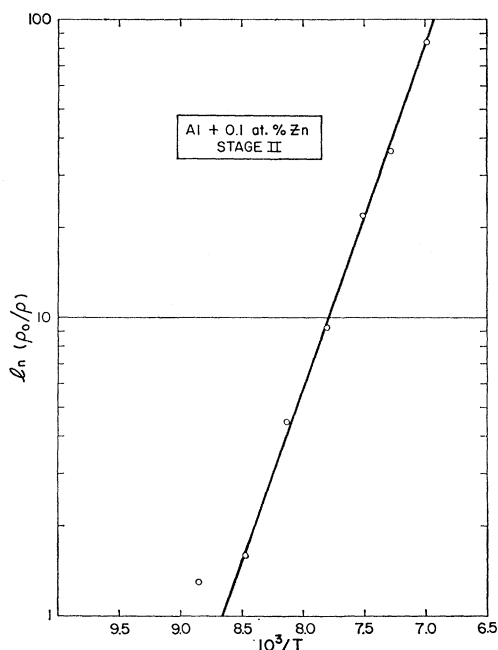
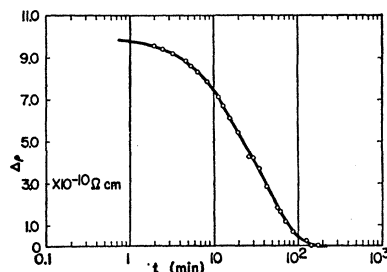


FIG. 13. Recovery of the electrical resistivity in Stage II in Al+0.1 at.% Zn analyzed for kinetics and activation energy. The method—the sequential isothermal method—is described in the text. This plot indicates a first-order process with an activation energy of about 0.22 eV. The data of Fig. 9 have been used here.

that the crowdions are sometimes trapped by zinc atoms without conversion to the $\langle 100 \rangle$ interstitial form and are released from such traps in Stage II, resuming their search for vacancies. Evidently copper atoms do not trap crowdions.

With this model it appears possible to explain the suppression of Stage I recovery by zinc and copper, the relatively large magnitude of Stage II in the zinc-doped material and the absence of Stage II due to interstitial trapping by copper atoms in the copper-doped material. The most complete absence of Stage II recovery in Al+0.1 at.% Cu is still, at first glance, surprising. One might expect recovery in this alloy comparable to that

FIG. 14. A study of the isothermal recovery of electrical resistivity of Al+0.1 at.% Zn in Stage II. This curve was constructed from the isochronal data of Fig. 9 with a temperature correction procedure described in the text.



observed in the pure material. The suppression of Stage II in this alloy we again ascribe to dynamic defocussing. That is, crowdions which traverse long distances in pure aluminum during irradiation may be trapped during their migration by residual impurity atoms. With 0.1 at.% Cu atoms, the range is restricted and some crowdions are converted to $\langle 100 \rangle$ interstitials. Therefore, the probability of migrating crowdions being trapped by residual impurity atoms, presumably also present in the copper-doped sample, is significantly reduced.

There are two observations with respect to Stage II in Al+0.1 at.% Zn which deserve further attention. We have stated that the observation that Stage II is a first-order process indicates that the underlying mechanism is one in which interstitials are released from traps near zinc atoms. This appears, at first glance at least, to be in conflict with the calculations of Damask and Dienes.⁹ Their calculations show that if interstitials are released from relatively deep traps and migrate eventually to vacancies, present in equal concentration to that of interstitials, the resulting kinetics are closely second order in nature, rather than first order. We note that this model is not entirely applicable to the present

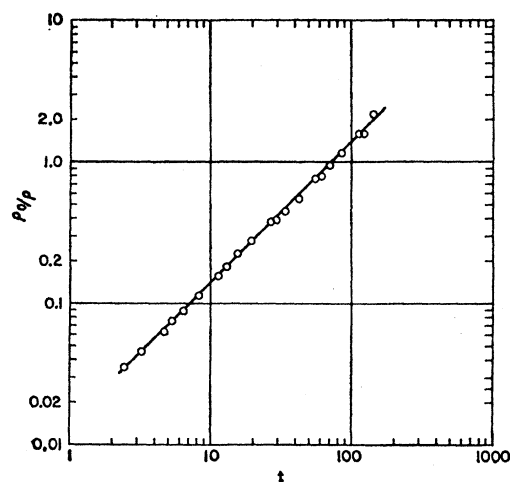


FIG. 15. A replot of the data of Fig. 14. The straight line with unit slope is indicative again of a first-order process in Stage II in Al+0.1 at.% Zn. The units of the abscissa are minutes at 138°K.

⁹ A. C. Damask and G. J. Dienes, Phys. Rev. **120**, 99 (1960).

experiment since an appreciable concentration of defects survive Stage II annealing. Thus, the condition that the concentration of vacancies equal the concentration of mobile interstitials is evidently not fulfilled.

Nevertheless, the Damask and Dienes theory is basically applicable if we assume that Stage II results from detrapping of crowdions and that these crowdions recombine with vacancies. The only modification necessary is to relax the condition that the concentration of vacancies equal the concentration of interstitials. The effect of this relaxation is to alter the order of kinetics governing the process; the process can be described as one in which the apparent order changes continuously during annealing from something between first and second order to a pure first-order process.

This can be demonstrated in the following manner. Consider a process in which interstitials of concentration i (and initial concentration i_0) migrate to vacant lattice sites, resulting in annihilation. In this simple treatment, we do not specify whether the interstitials are initially free or trapped—the activation energy governing the process is the migration energy in the first case and the sum of the migration plus the binding energy in the second case. We further specify that the vacancy concentration is in excess of the interstitial concentration by a constant amount, v_e . Then the rate equation governing this process is

$$di/dt = -\nu e^{-E/kT} i(i+v_e). \quad (5)$$

Integration of Eq. (5) gives

$$i = i_0 \frac{i+v_e}{i_0+v_e} \exp\left[-v_e \nu \exp\left(-\frac{E}{kT}\right)\right]. \quad (6)$$

Note that Eq. (5) describes a second-order reaction as $v_e \rightarrow 0$ and a first-order reaction as $v_e \rightarrow \infty$.

As may be seen from Fig. 9, Stage III in the Al+0.1 at.% Zn alloy is approximately three times as large as Stage II. In our model, this implies that $v_e \approx 3i_0$ and that the process does not deviate appreciably from first-order kinetics. It is quite possible that this deviation is not resolved in Fig. 13 despite the apparently satisfactory fit to a pure first-order reaction.

Consider now the number of jumps made by an interstitial in Stage II. As shown by Lomer and Cottrell,¹⁰ the number of jumps made by an interstitial in our model is:

$$j = \nu \bar{i} c^{-1} \exp[-E/kT], \quad (7)$$

¹⁰ W. M. Lomer and A. H. Cottrell, *Phil. Mag.* **46**, 711 (1955). A more exact expression than given in Eq. (7) would replace $c^{-1} \exp[-(E_m+B)/kT]$ by $(1-\beta c) \exp(-E_m/kT) / [1-\beta c + \beta c \exp(B/kT)]$, where β is the number of sites near a trapping atom in which the interstitial may be trapped. In the limit $\beta c \exp(B/kT) \gg 1$, the more simple expression may be used. In the present case, $\beta c \exp(B/kT) \approx 1$ in Stage II. The error in the use of the simpler expression is not serious, however, considering the uncertainties in the values of ν and \bar{i} .

where \bar{i} is a characteristic time for defects to migrate to a sink, taken here as 10^8 sec at $T=138^\circ\text{K}$; using the measured activation energy, $E=E_m+B=0.225$ eV, and $\nu \approx 10^{12}$ sec⁻¹ the number of jumps is about 10^{10} . (B is the binding or trapping energy of an interstitial due to a Zn atom.) Once again according to Lomer and Cottrell, the number of jumps required by a crowdion to reach a sink is $(\alpha z c)^{-2}$, where $\alpha = \frac{1}{2}$ and z is the coordination number. The sink concentration, c , is about $2-3 \times 10^{-6}$, from this expression. This is consistent with the concentration which may be predicted from Fig. 9. The magnitude of Stage II is about 10^{-9} $\Omega\text{-cm}$. Using the value of ρ_F adopted previously, we again deduce a value of $c = 3 \times 10^{-6}$.

In this model, the binding energy, B , is known once the free migration energy E_m , is available. Unfortunately, E_m is not yet established. However, we shall take $E_m = 0.12-0.13$ eV, using the data of Herschbach.¹¹ This then implies that $B \approx 0.1$ eV.

Within the proposed model, the mechanism for Stage III is evident. We suggest that $\langle 100 \rangle$ interstitials become mobile and primarily annihilate with vacancies, leading to a second-order reaction. The free migration energy for $\langle 100 \rangle$ interstitials is then 0.45 eV. Equation (7) may then be applied to determine the number of jumps made by such interstitials, with the removal of the c^{-1} factor and with the understanding that E now represents the free migration energy of this interstitial. The predicted number of jumps in pure Al is about 10^6 . This is again about the expected number of jumps since the defect concentration involved in Stage III is about 3×10^{-6} .

Before considering alternative models, it is appropriate to consider other related experiments to ascertain whether these experiments point to any discrepancies in our model. Probably the experiment most directly related to the present one is the neutron irradiation of aluminum performed by McReynolds, *et al.*¹² These investigators observed a major recovery of electrical resistivity and critical shear stress in the Stage III temperature region. They attempted to fit the resistivity isothermal recovery curve to first-, second-, and third-order processes and decided that a second-order reaction best fit the data, although considerable deviation was indicated. Using smoothed-out second-order plots, they can be deduced an activation energy of 0.55 eV. This same value was also deduced from the critical shear stress measurements.

We have re-examined their resistivity measurements and believe that the value 0.55 eV is subject to modification. Since McReynold's method for computing the activation energy from resistivity data involved a smoothing procedure assuming second-order kinetics, it seems likely that some error may be incurred. To

¹¹ K. Herschbach (to be published); see also *Bull. Am. Phys. Soc.* **7**, 171 (1962).

¹² A. W. McReynolds, M. McKeown, and D. B. Rosenblatt, *Phys. Rev.* **98**, 418 (1955).

some extent this error may be avoided by evaluating the energy differently. In this method, the shift in the three isothermal recovery curves (see Fig. 2 of McReynold's paper) along the abscissa, $\ln t$, is also a measure of the activation energy as implied by Eq. (A3) of the Appendix. We have estimated the energy by this method, using their data. We have analyzed the time shift between the isothermal curves for recovery at -40 and -60°C and find a value of 0.45 eV, in excellent agreement with the energy found in the present experiment. We find an energy of 0.52 eV, using the curves taken at -60 and -80°C but believe this value to be less reliable since a large portion of the curve at -80°C deviates from second-order, as shown by the authors. Furthermore, we do not believe that the critical shear stress measurements are suitable for precisely evaluating the activation energy due to the large amount of scatter in the data. Perhaps the most important criticism of the 0.55 eV value stems from a calculation of the number of jumps of the migrating defect. We estimate about 10^2 jumps. This appears to be at least two orders of magnitude too small for a second-order process.

Most recently measurements have been made of resistivity recovery in deformed aluminum by Frois and Dimitrov¹³ and by Panseri, Ceresara and Federighi.¹⁴ Both groups deduce activation energies for recovery in the Stage III region of 0.55 – 0.58 eV. Unfortunately, only abstracts of these papers are available so that the manner in which the energy is calculated is not known. However, we are again confronted by the problem of understanding the small number of jumps made by the defect in Stage III if we accept these relatively high values of activation energy.

The aluminum quenching experiments may also be cited. Presumably the best determination of the migration of energy of vacancy in aluminum is due to DeSorbo¹⁵: 0.65 ± 0.06 eV. The recent determination of the activation energy of self-diffusion,¹⁶ taken together with the high-temperature equilibrium measurements of Simmons and Balluffi,¹⁷ indicate that the most probable value of the vacancy migration energy is about 0.7 eV. It appears obvious that Stage III is not due to free vacancy migration.

¹³ C. Frois and O. Dimitrov, in Conference on Recovery of Metals, Delft, Holland, 1962 (unpublished).

¹⁴ C. Panseri, S. Ceresara, and T. Federighi, in Conference on Recovery of Metals, Delft, Holland, 1962 (unpublished); also private communication. *Note added in proof.*—Since submission of this article, we have been privileged to read a prepublication report of this work. It is apparent from this account that the activation energy for the process observed after neutron irradiation is quite different than the activation energy for Stage III after electron irradiation—Federighi *et al.* report 0.60 ± 0.01 eV. Our reservations concerning the energy value deduced by McReynolds *et al.* appear to be, at least in part, unjustified.

¹⁵ W. DeSorbo and D. Turnbull, Phys. Rev. **115**, 560 (1959); see also references therein.

¹⁶ T. S. Lundy and J. F. Murdock, J. Appl. Phys. **33**, 1671 (1962).

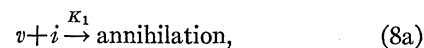
¹⁷ R. O. Simmons and R. W. Balluffi, Phys. Rev. **117**, 52 (1960).

We now consider other models for the recovery reported here. First we may eliminate the possibility that divacancies are the mobile defect in Stage III following electron irradiation. The concentration of divacancies formed directly during irradiation should be considerably less than 20% of the total vacancy concentration. Additional divacancies can only be formed by the migration of single vacancies. Since the migration energy of single vacancies is about 0.7 eV, we anticipate no formation divacancies in this manner. Thus, Stage III annealing, if divacancies were the mobile defect, should account for less than 20% of the resistivity increment due to irradiation which persists up to Stage III and the kinetics should not follow second order since the sink concentration (including single vacancies) would be in excess of the concentration of migrating defects.

The model we have proposed is a two-interstitial model. We now explore the various possible models assuming that only one form of interstitial is stable. There appear to be four possible single interstitial models, which we distinguish by the following possible Stage III processes

- (a) Break up of interstitial clusters, formed by interstitial agglomeration during Stage I and Stage II migration.
- (b) Migration of interstitial clusters, again formed by interstitial agglomeration at lower temperatures.
- (c) Release of interstitials from trapping positions near dislocations, the interstitials having been trapped during previous migration.
- (d) Release of interstitials from trapping sites near impurity atoms, the interstitials having been trapped during previous migration.

Model (a) may be ruled out on the basis of the order of the kinetics which would govern such a process. To see this, consider the case of dimer (di-interstitial) break up, ignoring higher order interstitial clusters. The kinetic reactions which describe the process are



where i , v , and δ are the free interstitial, vacancy, and cluster concentrations, respectively. The differential equations governing these reactions are

$$dv/dt = -K_1vi, \quad (9a)$$

$$di/dt = -K_1vi - K_2i^2 + K_3\delta, \quad (9b)$$

$$d\delta/dt = K_2i^2 - K_3\delta, \quad (9c)$$

where K_3 and $K_1 = K_2$ are the reaction rate constants, including the usual Boltzmann temperature dependence.

To determine the approximate order of reaction, we

make the following approximations, which should apply particularly well to Stage III in this model:

$$di/dt \simeq 0, \quad v \gg i, \quad v \simeq 2\delta. \quad (10)$$

With these approximations, it follows that $i \simeq K_3/2K_1$. The resistivity measurements, in this model, record the annihilation of equal numbers of vacancies and interstitials, so that the rate of decay of the vacancy concentration may be examined for the order of reaction:

$$dv/dt = -K_1v(K_3/2K_1) = -(K_3/2)v, \quad (11)$$

a first-order process. The inclusion of higher order interstitial clusters and their breakup would not alter this argument significantly.

Model (b) does approximate to a second-order reaction. Furthermore, there has been a fair amount of support for the idea that dimer formation is an important process during interstitial migration, despite the fact that one might intuitively expect a repulsion between interstitials, rather than an attraction, since the strains introduced by interstitials (particularly if the interstitial configuration is highly local) are highly compressive. In this regard, Eshelby's calculations¹⁸ indicate that these intuitive ideas may be misleading and that attraction is possible.

There are at least three experiments which may support a model in which dimer formation is important in some materials. Corbett and Walker,⁵ in analyzing the recovery of resistivity of copper in Stage I following electron irradiation, concluded that the probability of dimer formation is approximately equal to that of interstitial-vacancy annihilation (assuming random distribution of interstitials and vacancies). The recovery of gold following low-temperature electron irradiation, as observed by Ward and Kauffman¹⁹ and by Bauer, DeFord, Koehler, and Kauffman,²⁰ may also be interpreted with the inclusion of dimer formation, but this is somewhat premature since the studies of gold have not proceeded sufficiently far as yet. Most directly, electron microscopy following neutron irradiation²¹ appears to show the presence of interstitial clusters.

Despite these evidences for the possible importance of dimers, we do not believe that Stage III should be attributed to dimer migration. For example, it is very difficult to see why the presence of zinc or copper in aluminum should promote the formation of dimers; yet this is a necessary conclusion on the basis of the data in the present experiment. A similar argument can be made in copper where it has been shown that Stage III is enhanced in magnitude by pre-irradiation deformation. Here one would have to assume that dislocations catalyze dimer formation; again an unlikely possibility.

¹⁸ J. D. Eshelby, *Acta Met.* **3**, 487 (1955).

¹⁹ J. B. Ward and J. W. Kauffman, *Phys. Rev.* **123**, 90 (1961).

²⁰ W. Bauer, J. DeFord, J. S. Koehler, and J. W. Kauffman, *Phys. Rev.* **128**, 1497 (1962).

²¹ D. J. Mazey, R. S. Barnes, and A. Howie, *Phil. Mag.* **7**, 1861 (1962).

We next turn to model (c). Once again the observation of second-order kinetics is consistent with this model. There are two serious objections to the model, however. First, it is again difficult to see why the presence of zinc or copper in aluminum should enhance the number of interstitials which reach dislocations and then are released from dislocations in Stage III, unless the dislocation density is higher in the alloyed material than in the pure material. Second, measurement of elastic moduli changes of copper following electron irradiation and subsequent thermal treatment indicate that point defects arrive at dislocations in Stage III, rather than depart from dislocations.

Model (d) is the most likely explanation of Stage III in a one-interstitial model. This model was first proposed by Hasiguti²² and given additional credence by the calculations of Damask and Dienes,⁹ as discussed previously. There are, however, some experimental observations which are difficult to reconcile with this model. We note first that, on the basis of the present experiment, the impurity (or impurities) which is presumed to give rise basically to Stage III in "pure" aluminum is quite similar to copper and zinc in its trapping characteristics. While not inconceivable, this appears unlikely. Notice, for example, the difference between the effects of copper and zinc in aluminum in Stage II. Furthermore, Corbett and Walker have pointed out that, in copper, the fraction of resistivity change which persisted above Stage I was constant even though they varied their initial defect concentration from about 1×10^{-6} to 2×10^{-5} in the presence of an impurity concentration of about 1×10^{-6} .

The above discussion of possible recovery models is certainly not exhaustive. Nevertheless, we are led to the belief that the two-interstitial model is most consistent with the present observations and other pertinent observations to which we have referred. It may be valuable to make one further point for the purpose of clarification. While we have ruled out the possibility that divacancies play a significant role in Stage III after electron irradiation (at relatively low energies), it is not unlikely that divacancies play a more important role in recovery in the Stage III temperature region following plastic deformation, quenching, or irradiation with more massive or more energetic particles.

CONCLUSIONS

The following observations were made in the present work:

(1) Stage I in pure Al is similar, at least qualitatively, to Stage I in pure Cu.

(2) Impurities, copper and zinc in particular, suppress Stage I recovery.

²² R. R. Hasiguti, *J. Phys. Soc. Japan* **15**, 1807 (1960).

(3) Stage III in pure aluminum obeys second-order kinetics, similar to Stage III in pure copper, with an activation energy of 0.45 eV.

(4) Stage III in Al+0.1 at.% Zn obeys second-order kinetics with the same energy as observed in pure Al.

(5) For equal amounts of irradiation, Stage III is larger in Al+0.1 at.% Zn than in pure Al and is shifted to lower temperatures. The shift can be accounted for taking into account the different defect concentration implied by the unequal magnitudes of Stage III in the two cases and the observed second-order kinetics.

(6) Stage II in Al+0.1 at.% Zn obeys first-order kinetics, within the present accuracy. The activation energy is 0.22 eV. Stage II is considerably smaller in pure Al and is essentially absent in Al+0.1 at.% Cu.

From these observations one may directly exclude the following mechanisms to account for Stage III recovery following relatively low energy electron irradiation.

(1) Vacancy migration. The activation energy governing Stage III is too low.

(2) Divacancy migration. The energy of the bombarding electrons is too low to produce any appreciable concentration of divacancies.

(3) Dimer (di-interstitial) breakup. The kinetics of Stage III are in conflict with such a model.

The correct model for Stage III recovery appears to be limited then to the following possibilities:

(1) Dimer migration.

(2) Release of interstitial from traps near unspecified impurity atoms.

(3) Release of interstitials from traps near dislocations.

(4) Migration of a second type of interstitial, the first type having migrated in Stage I.

These last four models have been further compared. We believe the latter model fits the present observations and other related experimental data in the most consistent manner.

This model is compatible with and augments the two interstitial model previously proposed to explain recovery in Cu.

APPENDIX

In the regime of chemical rate theory, the rate of decay of a species of concentration, c , is usually written as

$$dc/dt = -\nu Pc^\gamma \exp(-E/kT), \quad (\text{A1})$$

where E is a governing activation energy, ν is the attack frequency (i.e., the number of times per second in which the defect attempts to change position), and P is the probability that, if the jump is successfully made, the defect will be removed from the lattice. As written, Eq. (A1) lends itself directly to the application in which isothermal measurements are made (i.e., where T is

maintained constant). More generally, if the temperature is programmed suitably, the dependence of T on time, t , is known and Eq. (A1) can be appropriately integrated.

To discuss the sequential isothermal method used in the text, we rewrite the above equation as

$$dc/d\tau = -\nu c^\gamma P, \quad (\text{A2})$$

with

$$\tau = t e^{-E/kT}. \quad (\text{A3})$$

When the reaction equation is written in the above manner, it becomes clear that, if the activation energy is known, a pseudoisothermal curve can be constructed by correcting the time t spent at temperature T to the equivalent time t_0 spent at an arbitrary temperature T_0 using an expression, which follows from Eq. (A3):

$$t_0 = t \exp \left[\frac{E}{k} \left(\frac{1}{T_0} - \frac{1}{T} \right) \right]. \quad (\text{A4})$$

The utility of a method which involves a time correction lies in the fact that the accuracy of purely isothermal measurements is limited by practical experimental difficulties. In order to obtain data at short annealing times so that time uncertainty is reduced, it is necessary to anneal the sample at low temperatures. In this case it becomes practically impossible to follow the annealing to sufficiently long times to study the latter portion of recovery, particularly as the order of reaction increases. If the temperature of anneal is increased to allow examination of the latter portion of recovery, the early annealing data are lost.

These difficulties are circumvented with the use of isochronal techniques, where the entire recovery process can be conveniently studied. However, there is a distinct disadvantage in the isochronal technique in that the activation energy must be known before the reaction kinetics can be analyzed. In the present work, we have used primarily the combined isothermal-isochronal technique of Meechan and Brinkman. This technique requires two samples, which may be a disadvantage in many cases. In such cases, the sequential isothermal technique becomes particularly advantageous. In this technique, several data points are obtained at each temperature. The activation energy can then be determined by the well known slope-change method for it follows from Eq. (A1) that the ratio of the time decay of defect concentration at an instant when the temperature is changed from T_1 to T_2 is

$$R = \frac{(dc/dt)_{T_1}}{(dc/dt)_{T_2}} = \exp \left[-\frac{E}{k} \left(\frac{1}{T_1} - \frac{1}{T_2} \right) \right], \quad (\text{A5})$$

so that

$$E = \frac{kT_1T_2}{T_1 - T_2} (\ln R). \quad (\text{A6})$$

The feature of the sequential isothermal method is

that, once E is determined, all the data points taken at each temperature are used in a subsequent reaction rate computation and the analysis can be applied over essentially all of the recovery process.

It should be noted that this analysis applies only in the case in which a single rate process is involved. The

situation becomes more complicated in the case that two or more processes are occurring. At the same time it may be noted that processes more complex than envisioned in Eq. (A1) may be analyzed by the sequential isothermal method providing that the only explicit time dependence is that given in Eq. (A3).

Infrared Reflectivities of Magnesium Silicide, Germanide, and Stannide*

D. McWILLIAMS† AND D. W. LYNCH

*Institute for Atomic Research and Department of Physics,
Iowa State University, Ames, Iowa*

(Received 14 February 1963)

The room-temperature reflection spectra of Mg_2Si , Mg_2Ge , and Mg_2Sn have been measured at wavelengths between 20 and 50 μ . Reststrahl reflectivity peaks were observed at 36 and 45 μ for Mg_2Si and Mg_2Ge , respectively, and a rising reflectivity in Mg_2Sn is estimated to peak at about 54 μ . The occurrence of peaks indicates that these compounds are partly ionic. The reflection spectra are more like those of the alkali halides than those of the III-V semiconducting compounds. If a simple damped harmonic oscillator is used to describe the reststrahl mode, the three Mg compounds have the same force constant for this mode. Values of dielectric constants and effective charges are estimated for Mg_2Si , and are used to evaluate a previous analysis of electron mobility in this compound. Effects of free carriers on the reflectivity of Mg_2Ge indicate that the effective masses are in rough agreement with the results of transport measurements.

INTRODUCTION

MAGNESIUM silicide, germanide, and stannide are cubic semiconducting compounds with the antiferroite structure. The most recent work on the electrical properties of¹ Mg_2Si and² Mg_2Ge indicates that optical mode scattering is important at room temperature. Morris *et al.* found a reasonable fit of their mobility data with a curve of optical mode-limited mobility versus temperature for longitudinal optical-mode phonons with a characteristic temperature of 400°K. For Mg_2Ge a characteristic temperature of 200°K was assumed. An optical dielectric constant of 19 resulted for Mg_2Si . The mobilities of carriers in Mg_2Sn have not been analyzed in such detail, but this compound is believed to be less ionic than Mg_2Si or Mg_2Ge .³ Reststrahl reflectivity peaks are expected to be observable in crystals in which optical mode scattering is important. The present set of measurements was undertaken to partly characterize the optical mode lattice vibrations in these compounds. By varying the purity of the crystals some information on carrier effective masses might be obtained, but because of the carrier densities obtained and the rather large effective masses ($0.2m_0$ to

$1.3m_0$),^{1,2,4} the effects of the carriers in our samples should not be great in the wavelength region covered.⁵

EXPERIMENTAL DETAILS AND RESULTS

All samples were cleaved faces of single crystals. Polished samples (not etched after polishing) showed a reduced reststrahl peak and were not used. The cleaved faces were not always perfectly plane but consisted of many parallel planes connected by steps. It is estimated that this effect reduced the reflectivity of these samples only a few percent, if at all.

The measurements were made at room temperature at a 12° angle of incidence. Light reflected from the sample or from an aluminum mirror used as a standard passed through a Perkin Elmer 160 fore-prism unit used as a prism monochromator with a thermocouple detector. NaCl, KBr, and CsI prisms were used with appropriate filters. For wavelengths below 30 μ the scattered light was less than 1%. The scattered light rose gradually to about 20% at 47 μ . Corrections based on measurements of scattered light were applied to all data. The corrected reflectivities should be in error by less than 0.05 at 47 μ due to scattered light. Sample-to-sample differences are probably due to differences in surface condition and carrier concentration.

The near normal reflectivities of Mg_2Si , Mg_2Ge , and

* Contribution No. 1274. Work was performed in the Ames Laboratory of the U. S. Atomic Energy Commission.

† Present address: Autonetics, a Division of North American Aviation Inc., Anaheim, California.

¹ R. G. Morris, R. D. Redin, and G. C. Danielson, Phys. Rev. **109**, 1909 (1958).

² R. D. Redin, R. G. Morris, and G. C. Danielson, Phys. Rev. **109**, 1916 (1958).

³ J. P. Suchet, J. Phys. Chem. Solids **21**, 156 (1961).

⁴ R. F. Blunt, H. D. R. Frederikse, and W. R. Hosler, Phys. Rev. **100**, 663 (1955).

⁵ T. S. Moss, *Optical Properties of Semi-Conductors* (Butterworths Scientific Publications Ltd., London, 1959), pp. 29–33.